

# Experimental diffusion measurement of light and heavy water mixing using neutron radiography

By A. Zeilinger, M. Suleiman and H. Rauch

Atominstitut der Österreichischen Universitäten, Wien, Austria

## Abstract

Studies on the  $H_2O-D_2O$  diffusion process using neutron radiography are herein reported. It is shown that the  $H_2O-HDO-D_2O$  concentration profiles obtained experimentally are characterized by an universal dependence on the distance from the initial separation face divided by the square root of the diffusion time. Furthermore, numerical values describing the rate of mixing have been determined.

## Zusammenfassung

Neutronenradiographische Untersuchung des  $H_2O-D_2O$ -Diffusionsprozesses  
Über neutronenradiographische Untersuchungen des  $H_2O-D_2O$ -Diffusionsprozesses wird berichtet. Es wird gezeigt, daß die durch das Experiment erhaltenen  $H_2O-HDO-D_2O$ -Konzentrationsprofile durch eine allgemeine Abhängigkeit von der Entfernung von der ursprünglichen Trennfläche, dividiert durch die Wurzel aus der Diffusionszeit, charakterisiert werden können. Numerische Werte, die das Durchmischungsverhalten beschreiben, wurden bestimmt.

## INIS DESCRIPTORS

NEUTRON RADIOGRAPHY  
WATER  
HEAVY WATER  
MIXTURES  
DIFFUSION

DEUTERIUM COMPOUNDS  
QUANTITY RATIO  
TIME DEPENDENCE  
MIXING

## 1. Introduction

One of the most efficient applications of neutron radiography is based on the fact, that the neutron attenuation coefficient of the hydrogen isotope  $^1H$  is exceptionally high, therefore, hydrogen may be detected by neutron radiography under experimental conditions where X-ray or  $\gamma$ -ray radiography fails to give meaningful results [1; 2]. Some typical applications in this field are the inspection of metal adhesives, explosives, hydride in metals and similar problems [3]. The first application of neutron radiography on the investigation of hydrogen diffusion was reported by Chountas and Rauch [4]. They studied the  $H_2O-D_2O$  diffusion process and found some discrepancies with simple diffusion theory. Later on more detailed results including also the methanol diffusion process were obtained [5]. A more detailed study of the phenomena required some additional experiments were made and are here presented.

## 2. Experimental method

For the inspection of non-radioactive samples the direct exposure technique can be used. Here a photographic film is in contact with a Gd-foil and is exposed to the neutron beam which has passed through the object. The film is blackened by internal conversion electrons following the capture of neutrons by gadolinium. Fig. 1 shows the setup at the beam

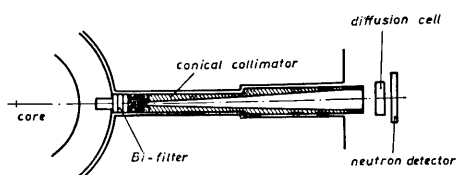


Fig. 1: Neutron radiography installation at the TRIGA reactor Vienna

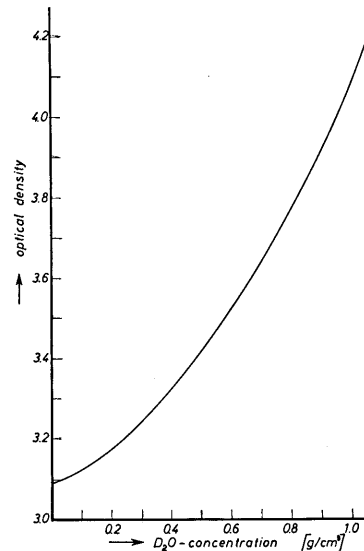


Fig. 2: Calibration curve: optical density as a function of the mixing ratio of  $H_2O-D_2O$

hole of the TRIGA Mark II reactor, Vienna. The gamma component of the beam is reduced by an 8 cm thick polycrystalline Bi-filter. The conical collimator provides an effective "point source" of neutrons. The inner diameter for our experiments was 17 mm. The diffusion process was studied using an Al-container with a 5 mm space for the water which was held at a constant temperature of  $25 \pm 0.01$  °C. To avoid any condensation of water at the outer side of the aluminium and for thermal isolation, the container was surrounded by an evacuated jacket. To obtain quantitative results, a calibration was made by radiographing a series of standard mixtures (0, 10...90, 100%  $D_2O$ ). For each mixture three radiographs were made and the mean value was used. At the beginning of each diffusion process the container was filled up to half its height with  $D_2O$ , on to which a layer of  $H_2O$  was very carefully deposited using an inverted tube, Fig. 2, to avoid any inadvertant mixing of the two liquids.

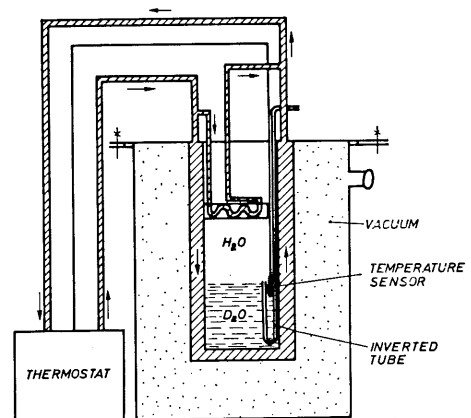


Fig. 3: The diffusion cell with the inverted tube used for the deposition of  $H_2O$  on to  $D_2O$  without inadvertant mixing

Afterwards, radiographs were taken at different times. The exposure time of all radiographs was 5 minutes. Fig. 3 shows a typical neutron radiograph. The radiographs were scanned using a microdensitometer with a slit width of 75  $\mu\text{m}$  and 2.5 mm in length. This slit was oriented parallel to the initial separation face of the two liquids. All films used were taken from the same film package (OSRAY TA T4 DW film) and were developed together under identical conditions.

### 3. Results

The calibration curve is shown on Fig. 4. We point out, that on the abscissa we have not plotted the actual concentration of  $\text{D}_2\text{O}$  for the following reasons. Because of the dynamic equilibrium,

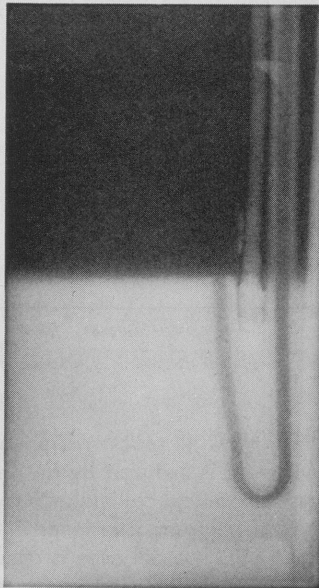
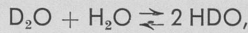


Fig. 4: Neutron radiograph of the diffusion cell taken before the measurements to adjust the inverted tube and the temperature sensor. Note, that the tube is filled with  $\text{H}_2\text{O}$

each mixture of heavy water and light water is accompanied by a certain concentration of HDO. The amount of HDO can be determined using the law of mass action governing the concentrations  $C$  as follows:

$$\frac{C_{\text{HDO}}^2}{C_{\text{H}_2\text{O}} \cdot C_{\text{D}_2\text{O}}} = K.$$

Therefore the calibration curve represents the optical density as a function of the volumes of  $\text{D}_2\text{O}$  and  $\text{H}_2\text{O}$  before mixing. This calibration curve can be used to convert the microdensitometer readings of the radiographs of the diffusion process to concentration profiles. By this method one obtains concentration profiles as shown in [5]. Any evaluation of these profiles is readily accomplished by assuming that the system is spatially unlimited [6], which is fulfilled in our case because

$$2Dt \ll L^2$$

where  $D$  is the diffusion coefficient,  $t$  is the diffusion time and  $L$  is the linear expansion of the system in the direction of diffusion. The concentration profiles then can be used to determine the diffusion coefficient as a function of concentration. This procedure was repeated in the present work thus

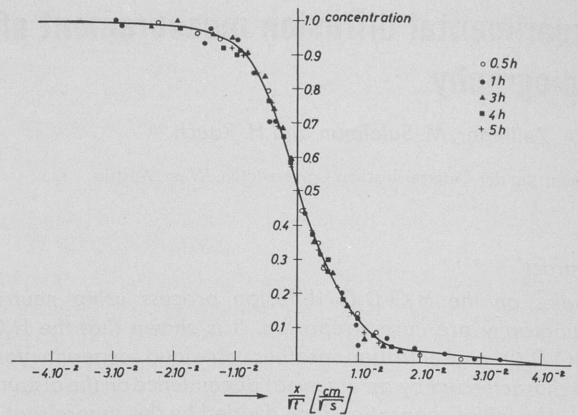


Fig. 5: Spread of the initial  $\text{D}_2\text{O}$  distribution by the diffusion process. The ordinate does not show actual concentrations but mixing ratios of compositions giving the same optical density. For different values of  $x/\sqrt{t}$  one obtains the same curve

confirming the previously found form of the concentration dependence. Furthermore, we used the observation that for most diffusion processes the concentration is a function of  $x/\sqrt{t}$  where  $x$  is the distance from the original border of the two substances and  $t$  is the time elapsed since the beginning of the diffusion process [6]. When this holds, all concentration profiles obtained at different diffusion times coincide when plotted as a function of  $x/\sqrt{t}$ . Fig. 5 shows this "normalized" concentration profile for the diffusion process investigated and clearly confirm the validity of the  $x/\sqrt{t}$  dependence. From this curve the concentrations of  $\text{H}_2\text{O}$ ,  $\text{D}_2\text{O}$  and HDO were determined using the law of mass action with  $K = 3.96$  [7] for any  $x$  and any  $t$ . Fig. 6 shows the concentrations as a function of  $x/\sqrt{t}$ . As can be seen for  $|x/\sqrt{t}| > 1.5 \times 10^{-2} \text{ cm s}^{-1/2}$  only two components coexist whereas in the intermediate values we have coexistence of  $\text{H}_2\text{O}$ , HDO and  $\text{D}_2\text{O}$ . From this figure the amount of HDO per unit area of the initial separation face present as a consequence of the diffusion process was found to be

$$m_{\text{HDO}} = 1.13 \cdot 10^{-2} \sqrt{t} \quad (\text{g/cm}^2)$$

This number was obtained by integration of the HDO-concentration profile. From that figure we get the rate of production of HDO as

$$\dot{m}_{\text{HDO}} = 5.6 \cdot 10^{-3} / \sqrt{t} \quad (\text{g/cm}^2 \text{ s})$$

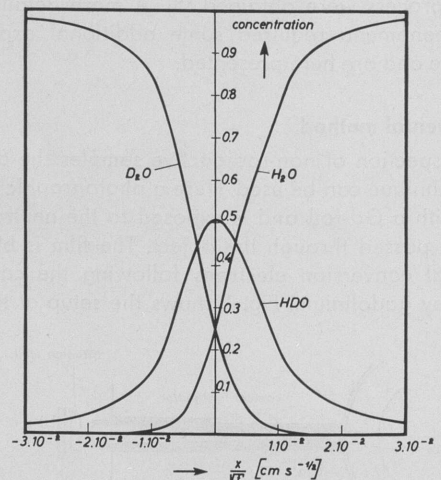


Fig. 6: Concentration profiles of  $\text{H}_2\text{O}$ , HDO and  $\text{D}_2\text{O}$  as a function of the "reduced distance" from the initial separation face between  $\text{H}_2\text{O}$  and  $\text{D}_2\text{O}$

that is, the production rate decreases with the square root of the diffusion time. These values are important in cases where  $H_2O$  and  $D_2O$  might mix such as in  $D_2O$ -moderated  $H_2O$ -cooled nuclear reactors and in heat exchangers of  $D_2O$ -cooled reactors.

#### 4. Concluding comments

We have used neutron radiography as the diagnostic tool to measure the diffusion process of light and heavy water. Both, a general characterization of the diffusion process has been identified and specific numerical values describing the mixing process have been evaluated. For that applications neutron radiography is superior to other techniques because the results can be obtained in principle by taking only one neutron radiograph of the diffusion process.

(Received on 28. 5. 1976)

#### Acknowledgement

Some useful comments by Prof. A. A. Harms are gratefully acknowledged.

#### References

- [1] Berger, H.: Neutron Radiography. Annual Review of Nuclear Science. Annual Reviews Inc., Palo Alto, California, USA, 1971
- [2] Rauch, H., G. Saringer: Materialprüf. **8** (1966) 134
- [3] A good survey of the present status of neutron radiography has been reported at the BNES Conference "Radiography with Neutrons" Birmingham, 1973. Proceedings: M. R. Hawkesworth (Ed.), London, British Nuclear Energy Society, 1975
- [4] Chountas, K., H. Rauch: Atomkernenergie **13** (1968) 444
- [5] Mannooussakis, M., H. Rauch, A. Zeilinger: paper no. 24, p. 143 in Ref. [3]
- [6] Jost, W., K. Hauffe: Diffusion-Methoden der Messung und Auswertung. Darmstadt: Dr. Dietrich Steinkopff Verlag 1972
- [7] Urey, H. C.: J. Chem. Soc. **1947**, p. 562

## Einführung in die Neutronenphysik

von Privatdozent Dr. Wolfgang Gläser, Karlsruhe  
(1973) VIII, 160 Seiten, 81 Abbildungen, 15 Tabellen; Format 11 x 17,5 cm;  
kartoniert-cellophanisiert; DM 16,80

THIEMIG-  
TASCHENBÜCHER  
BAND 39

### Inhaltsübersicht in Kurzfassung:

**Entdeckung und Eigenschaften des Neutrons** · Historisches · Eigenschaften freier Neutronen.

**Erzeugung von Neutronen** · Radioaktive ( $\alpha, n$ )-Quellen · Photoneutronenquellen · Spaltneutronenquellen · Erzeugung von Neutronen mit Beschleunigern · Erzeugung von Neutronen mit Reaktoren.

**Der Begriff des Wirkungsquerschnittes** · Mikroskopische Wirkungsquerschnitte · Makroskopischer Wirkungsquerschnitt und mittlere freie Weglänge.

**Neutronendetektoren** · Ionisationskammern und Proportionabzählrohre für langsame Neutronen · Szintillationsdetektoren · Protonenrückstoß-Detektoren für schnelle Neutronen · Neutronennachweis durch Aktivierung.

**Wechselwirkung von Neutronen mit Materie** · Neutron-Proton-Wechselwirkung · Neutron-Neutron-Wechselwirkung · Kernwechselwirkung der Neutronen · Einfluß der chemischen Bindung auf die Neutron-Kernwechselwirkung · Neutron-Elektron-Wechselwirkung.

**Moderation und Diffusion von Neutronen** · Neutronenmoderation · Bremsdichte und Fermialter · Neutronendiffusion.

**Kernreaktionen mit Neutronen** · Studium der Kernstruktur · Erzeugung neuer Nuklide · Entstehung der Elemente.

**Streuung und Beugung von langsamen Neutronen** · Welleneigenschaften des Neutrons · Kohärente und inkohärente Streuung · Methoden der Neutronenbeugung · Untersuchung magnetischer Strukturen mit Neutronen · Erzeugung polarisierter Neutronen

**Unelastische Streuung langsamer Neutronen an kondensierter Materie** · Atombewegungen · Prinzip der unelastischen Streuung und experimentelle Methoden · Experimentelle Ergebnisse.

**Kernreaktoren** · Neutronenbilanz · Reaktoren endlicher Größe · Zeitverhalten eines Reaktors.

**Aktivierungsanalyse** · Grundlagen · Experimentelle Methoden.

**Anhang** · Sachverzeichnis.



VERLAG KARLTHIEMIG · POSTFACH 900740 · D-8000 MÜNCHEN 90